A Global Time-Dependent Model of Thunderstorm Electricity. Part I: Mathematical Properties of the Physical and Numerical Models

G. L. BROWNING

Scientific Computing Division, National Center for Atmospheric Research, Boulder, CO 80307

I. TZUR AND R. G. ROBLE

High Altitude Observatory, National Center for Atmospheric Research, Boulder, CO 80307*

(Manuscript received 17 September 1986, in final form 27 February 1987)

ABSTRACT

A time-dependent model that simulates the interaction of a thunderstorm with its electrical environment is introduced. The model solves the continuity equation of the Maxwell current density that includes conduction, displacement, and source currents. Lightning phenomena are neglected and the electric field is assumed to be curl free. Corona, convection, and precipitation currents are not considered in this initial study and their contribution to the source function is not specified explicitly. As a preliminary test of the model we assume that the storm is axially symmetric in spherical geometry, the conductivity depends only on the vertical coordinate, the ground is equipotential, and far from the thunderstorm region the horizontal electric field is zero. These assumptions are for computational efficiency only and can be relaxed in more realistic studies.

The mathematical energy method is applied to the continuity equation to determine boundary conditions that are sufficient to form a well-posed initial–boundary value problem. This ensures the existence of a physical solution that depends continuously on the initial and boundary data. Then analytic techniques are applied to study the dependence of the solution on the properties of the medium. There are two time scales of the problem that are analyzed and discussed: one determined by the background electrical conductivity and the other by the time dependence of the source function. The assumed source function, which represents a mechanism by which charge is separated inside the storm, contributes to a portion of the solution in which the ratio of the displacement current over the conduction current increases with decreasing altitude, i.e., in the lower atmospheric region the displacement current can have an important role in the electrical interaction between the storm and its environment. It is also demonstrated that the source function can induce temporal phase shifts in the solution, which are dependent on altitude.

To obtain details of the solution, which cannot be obtained by analytic techniques, a stable numerical approximation of the continuity equation is introduced and analyzed. The resulting numerical model is used to examine the evolution of the displacement and conduction currents during the charge buildup phase of a developing thunderstorm.

1. Introduction

In previous studies of the global electric circuit a quasi-static thunderstorm has been used to describe the time-averaged output current into the global circuit (Holzer and Saxon, 1952; Kasemir, 1959; Israel, 1973; Hays and Roble, 1979). Many of the basic properties of the interaction between the thunderstorm and its environment can be described by quasi-static models, e.g., the average current that flows from the thunderstorm into the global electric circuit, the role of the equalization layer, and the spatial variations of the electric field in the atmosphere (Tzur and Roble, 1985). The intensity of the electrical parameters of a real storm, however, changes with time and there is a need to consider the time-dependent interactions of a thunderstorm with its global electrical environment by using a time-dependent model. Recently, Nisbet (1983, 1985) has developed a time-dependent model of thunderstorm electricity and has presented results that describe the importance of various components of the Maxwell current including the displacement current. His model is based on the analysis of an analog network of electric circuits. Developments of new measuring techniques have also produced data on the variation of the total or Maxwell current density over the life history of a thunderstorm (Krider and Musser, 1982; Krider and Blakeslee, 1985; Holzworth et al., 1985).

The various types of current that are associated with the process of cloud electrification are also time-dependent during the storm. Among them are the con-

* The National Center for Atmospheric Research is sponsored by the National Science Foundation.

duction, displacement, charge separation, convection, precipitation, and corona currents. Therefore, a time dependent model is needed to study problems involved in thunderstorm electrification and the role of a thunderstorm as an electric generator in the global circuit. A suggestion that the Maxwell current density, J_M, is a relevant electrical quantity in the complex, time varying environment within, under, and near a storm was first made by Krider (1981), Blakeslee and Krider (1981, 1982, 1983) and Krider and Musser (1982). They suggested that a quasi-static situation is maintained with respect to the Maxwell current.

Bostrom and Fahleson (1977) characterize problems in atmospheric electricity as belonging to one of the following three classes: 1) quasi-static problems where the time derivative can be neglected; 2) problems that include the displacement current; and 3) problems that include an additional second-order term which arises from the magnetic effects generally associated with short-term intense current systems such as lightning. They used the Fourier transform to separate the electric field into spatial and temporal harmonics and studied each component separately. This approach was also used in studies of time dependent fields in a thunderstorm by Anderson and Freier (1969), Mann (1970), and Illingworth (1972).

In this study we consider the continuity equation of the Maxwell current which we discuss in section 2. The Maxwell current is assumed to be the sum of the conduction current, the displacement current, and a parameterized source function that represents the mechanism by which charge is separated in a thunderstorm. The electric field is assumed to be curl free. Lightning, precipitation, conduction, and corona currents are not considered. In section 3 we determine boundary conditions which can be used in conjunction with the continuity equation to form a well-posed initial–boundary value problem. This ensures continuous dependence of solutions on the initial and boundary data. In section 4 we analytically determine some mathematical and physical properties of various components of solutions of the initial–boundary value problem. The analysis indicates that the problem has two time scales, one determined by the background electrical conductivity and the other by the time variation of the source function. The inhomogeneous solution arising from the source function has properties which are completely different from those of the homogeneous solution. In particular, the forced solution has temporal phase shifts which depend on altitude. To obtain quantitative results we introduce a numerical method and study its properties in section 5. In section 6 we present the results of some simulations from the corresponding numerical model. This numerical case study examines the evolution of the displacement and conduction currents during the electrification of the storm and demonstrates their role in the interaction between the thunderstorm and its environment.

2. Description of the physical model

We introduce a time-dependent model of the electrical behavior of a thunderstorm interacting with its electrical environment. It is a model of the thunderstorm electric generator and affects the global conducting atmosphere in the layer between the earth's surface and the highly conducting ionosphere. The model represents the thunderstorm as a specified source function that separates charge at a given rate.

As described in the introduction, we limit our considerations to the basic components of the Maxwell current, namely, the conduction current, the displacement current, and the charge separation current. The other types of current, e.g., the corona current and the convection current, will not be considered in this paper.

The basic equation of our model is the continuity equation of the electric current

$$\nabla \cdot (\sigma \vec{E} + \epsilon \vec{E}_t + \vec{J}_S) = 0, \tag{2.1}$$

where σ is the electrical conductivity, $\vec{E}$ is the electric field vector, ϵ is the permitivity, t is the independent variable representing time, and $\vec{J}_S$ is the charge separation current that acts inside the storm and electrifies the cloud. An independent variable subscript on a dependent variable indicates partial differentiation with respect to that independent variable.

The divergence of the separation current can be written as a source function

$$S = \nabla \cdot \vec{J}_S, \tag{2.2}$$

where S has the dimension of the time rate of growth of space charge. Using (2.2) and the fact that the electric field is the gradient of the potential, i.e., $\vec{E} = -\nabla\phi$, Eq. (2.1) can be written as

$$\nabla \cdot (\sigma \nabla \phi + \epsilon \nabla \phi_t) = S. \tag{2.3}$$

The domain for (2.3) is similar to that used by Tzur and Roble (1985) except for spherical coordinates rather than cylindrical coordinates. The atmosphere is divided into two hemispheres which extend from the ground to a given altitude. One hemisphere includes the thunderstorm which acts to separate charge and the other represents the passive conjugate hemisphere which is charged by the output currents flowing from the thunderstorm. The boundary conditions are zero potential at the surface of both hemispheres and zero horizontal derivative of the potential at the lateral boundaries. The boundary condition at the top of the atmosphere allows current to flow freely along geomagnetic field lines between magnetic conjugate hemispheres and is handled similar to the representation used by Hays and Roble (1979).

As an initial test of the validity of the model, in this paper we will assume that the conductivity profile does not vary in the horizontal direction. The conductivity profile is the same used by Tzur and Roble (1985), except for the anisotropic region above about 65 km.

In that region we average the directional conductivities and use an isotropic profile. Near the ground we use a conductivity of 3×10^{-14} mho m^{-1} while in the highly conducting layer near an altitude of 90 km we use a conductivity of 10^{-4} mho m^{-1}.

3. Well-posedness of the initial–boundary value problem

In this section we want to consider the initial–boundary value problem for the linear equation

$$\nabla \cdot (\sigma \nabla \phi + \epsilon \nabla \phi_t) = S, \tag{3.1}$$

where ϵ is a positive constant and σ ($\sigma > 0$) and S are given functions of time and space. To show that (3.1) with suitable boundary conditions forms a well-posed problem, we must first show that there exists a sufficiently large class of solutions. We discuss how this may be accomplished in the Appendix. Second, we must show that the solutions depend continuously on the initial and boundary data. For time-dependent problems in other mathematical systems, e.g., symmetric hyperbolic systems, the energy method is used to prove continuous dependence on the data (e.g., Browning et al., 1980). Therefore, it is reasonable to apply the energy method to the initial–boundary value problem for (3.1) to try to determine boundary conditions that are sufficient for well posedness.

To apply the energy method we consider (3.1) in an arbitrary closed and bounded region V with boundary B. Multiplying (3.1) by ϕ and integrating over V we find that

$$\int_V \phi \nabla \cdot (\sigma \nabla \phi + \epsilon \nabla \phi_t) dV = \int_V \phi S dV. \tag{3.2}$$

Using product differentiation rules we can rewrite (3.2) as

$$\int_V [\nabla \cdot \phi(\sigma \nabla \phi + \epsilon \nabla \phi_t) - \nabla \phi \cdot (\sigma \nabla \phi + \epsilon \nabla \phi_t)] dV = \int_V \phi S dV. \tag{3.3}$$

Applying the divergence theorem and the Cauchy-Schwarz inequality (3.3) becomes

$$\begin{aligned}
\frac{1}{2}\epsilon \frac{\partial}{\partial t} \int_V \nabla \phi \cdot \nabla \phi dV &= -\int_V \phi S dV \\
&\quad - \int_V \sigma \nabla \phi \cdot \nabla \phi dV + \int_B \phi(\sigma \nabla \phi + \nabla \phi_t) \cdot n dB \\
&\leq \left(\int_V \phi^2 dV \right)^{1/2} \left(\int_V S^2 dV \right)^{1/2} + \int_B \phi(\sigma \phi_n + \epsilon \phi_{nt}) dB \\
&\leq \frac{1}{2} \int_V \phi^2 dV + \frac{1}{2} \int_V S^2 dV + \int_B \phi(\sigma \phi_n + \epsilon \phi_{nt}) dB \\
&\leq \frac{1}{2} C_1 \int_V \nabla \phi \cdot \nabla \phi dV + \frac{1}{2} \int_V S^2 dV \\
&\quad + \int_B \phi(\sigma \phi_n + \epsilon \phi_{nt}) dB, \qquad (3.4)
\end{aligned}$$

where n is the exterior normal and ϕ_n is the derivative of ϕ in that normal direction. To derive (3.4) we have also used the fact that

$$\int_V \phi^2 dV \leq C_1 \int_V \nabla \phi \cdot \nabla \phi dV \tag{3.5}$$

where C_1 is a constant (e.g., Courant and Hilbert, 1966). If we choose

$$\phi = 0, \tag{3.6}$$

$$\sigma \phi_n + \epsilon \phi_{nt} = 0, \tag{3.7}$$

or

$$\phi + \alpha(\sigma \phi_n + \epsilon \phi_{nt}) = 0 \quad (\alpha > 0), \tag{3.8}$$

then the surface integral on the right-hand side of (3.4) is nonpositive and we obtain the Gronwall inequality

$$I_t \leq \epsilon^{-1} C_1 I + \epsilon^{-1} \int_V S^2 dV, \tag{3.9}$$

where

$$I = \int_V \nabla \phi \cdot \nabla \phi dV. \tag{3.10}$$

We can integrate (3.9) to obtain the estimate

$$I(t) \leq e^{\epsilon^{-1} C_1 t} I(0) + \epsilon^{-1} \int_V \int_0^t e^{\epsilon^{-1} C_1 (t - \tilde{t})} S^2 d\tilde{t} dV. \tag{3.11}$$

The Sobolev norm is defined as

$$\|\phi\|_1^2 = \int_V (\phi^2 + \nabla \phi \cdot \nabla \phi) dV. \tag{3.12}$$

Using (3.5), (3.11), and (3.12) we obtain the estimate

$$\|\phi\|_1 \leq C_2 \left[e^{\epsilon^{-1} C_1 t/2} \|\phi|_{t=0}\|_1 + \epsilon^{-1/2} \left(\int_V \int_0^t e^{\epsilon^{-1} C (t - \tilde{t})} S^2 d\tilde{t} dV \right)^{1/2} \right], \tag{3.13}$$

where $C_2 = (1 + C_1)^{1/2}$. Equation (3.13) states that (3.1) in conjunction with any of the boundary conditions (3.6), (3.7), or (3.8) is a well-posed initial–boundary value problem. It is also possible to use inhomogeneous versions of the boundary conditions. In that case let f be any function that satisfies the boundary condition. Define the new variable $\phi = f + \phi'$. Substituting this expression for ϕ into (3.1) and into the inhomogeneous version of (3.6), (3.7) or (3.8) the resulting problem for ϕ' reduces to the homogeneous case we have already considered.

The proof of well-posedness holds for any number of spatial variables. However, in this paper we assume that the solution is axisymmetric in spherical coordi-

nates so that we only need to solve two-dimensional elliptic problems rather than the three-dimensional ones for the general case. Since we have also assumed that σ is only a function of the vertical coordinate r, the elliptic equation will be separable. These two assumptions allow us to compute the solution efficiently while retaining enough of the physics to determine if computations in three dimensions are required. For the restricted case (3.1) becomes

$$\nabla \cdot \sigma \nabla \phi + \epsilon \nabla \cdot \nabla \phi_t = S, \tag{3.14}$$

with the operator $\nabla \cdot g(r)\nabla$ (g an arbitrary function of r) defined by

$$\nabla \cdot g(r)\nabla h(r,\theta) = r^{-2}[(r^2 g h_r)_r + g(\sin\theta)^{-1}(\sin\theta h_\theta)_\theta].$$

Note that when $g = 1$ this is just the axisymmetric Laplacian operator in spherical coordinates. We consider (3.14) in the region

$$V = \{(r,\theta): r_{\text{ground}} \leqslant r \leqslant r_{\max}, 0 \leqslant \theta \leqslant \pi/2\}.$$

We assume that the surface of the earth is a conductor so that

$$\phi(r = r_{\text{ground}}) = 0. \tag{3.15a}$$

Since $r = r_{\max}$ represents the surface of the conjugate hemisphere,

$$\phi(r = r_{\max}) = 0. \tag{3.15b}$$

We are interested in solutions that have bounded derivatives. This requirement implies that at the axis of symmetry we must have

$$\phi_\theta(\theta = 0) = 0 \tag{3.15c}$$

to avoid a solitary unbounded term in (3.14). We assume no horizontal currents at the remaining lateral boundary, i.e., that

$$\phi_\theta(\theta = \pi/2) = 0. \tag{3.15d}$$

The boundary conditions (3.15a–d) are in the proper form for the energy proof to hold, i.e., the surface integral on the right-hand side of (3.4) is nonpositive, and we can conclude that (3.14) in conjunction with these boundary conditions is a well-posed initial–boundary value problem.

4. Properties of solutions based on analysis

The evolution of the solutions of (3.14) is determined both by the properties of the medium, i.e., the values of ϵ and σ, and the form of S. Before solving Eq. (3.14) in conjunction with the boundary conditions (3.15a–d) by a numerical method, we will use analytic methods to obtain information on the dependence of the solutions on the constant ϵ and the functions σ and S in a number of special cases. This information can be used to check the numerical model against a number of known solutions and to help the physical understanding of the numerical results in those cases where analytic solutions can not be derived.

We are interested in an isolated storm that begins in a quiescent atmosphere, i.e., we assume that $\phi = 0$ at $t = 0$. We will also assume that S has a Laplace transform. We apply the Laplace transform in time ($t \to s$) and the Legendre transform in latitude ($\theta \to n$) to (3.14) and (3.15) to obtain for sufficiently large s and each integer $n \geqslant 0$ the boundary value problem

$$(\sigma + \epsilon s)[\hat{\phi}_{rr} + 2r^{-1}\hat{\phi}_r - r^{-2}n(n+1)\hat{\phi}] + \sigma_r \hat{\phi}_r = \hat{S}, \tag{4.1a}$$

$$\hat{\phi}|_{r=0} = \hat{\phi}|_{r=\max} = 0, \tag{4.1b}$$

where $\hat{\phi}(n, r, s)$ denotes the transform of $\phi(\theta, r, t)$. Note that this transform can not be carried out when σ is also a function of latitude. Equation (4.1) can not be solved analytically for general σ. However there are a number of special cases where (4.1) can be solved and which give insight into properties of more general solutions of (4.1).

We begin with the assumption that σ is a constant. In this case (4.1a) can be written

$$(\sigma + \epsilon s)\hat{R} = \hat{S},$$

where

$$\hat{R} = [\hat{\phi}_{rr} + 2r^{-1}\hat{\phi}_r - r^{-2}n(n+1)\hat{\phi}].$$

In physical space this means that we can solve for the time dependence of the solution separately from the spatial dependence, i.e., we first solve the initial value problem

$$\sigma R + \epsilon R_t = S, \tag{4.2a}$$

$$R|_{t=0} = 0, \tag{4.2b}$$

and then the boundary value problem

$$\nabla^2 \phi = R, \tag{4.3a}$$

$$\phi|_{r=0} = \phi|_{r=\max} = 0, \tag{4.3b}$$

$$\phi_\theta|_{\theta=0} = \phi_\theta|_{\theta=\pi/2} = 0, \tag{4.3c}$$

at those times of interest.

The general solution of (4.2) is given by

$$R = e^{-\epsilon^{-1}\sigma t}R(t=0) + \epsilon^{-1}e^{-\epsilon^{-1}\sigma t}\int_0^t e^{\epsilon^{-1}\sigma \tilde{t}} S d\tilde{t}. \tag{4.4}$$

As expected the homogeneous part of the solution decays with a time constant of $\epsilon\sigma^{-1}$. In the case that σ is a function of r we expect the homogeneous part of the solution to decay much faster at higher altitudes where the conductivity is much larger than near the surface. If S is a constant then the solution is

$$R = e^{-\epsilon^{-1}\sigma t}R(t=0) + \sigma^{-1}(1 - e^{-\epsilon^{-1}\sigma t}),$$

and the time scale is essentially that of the homogeneous solution. S can, however, vary with time. In this case the solution also has a part with a time scale determined by the forcing. The easiest way to see this is to assume that S consists of a single frequency, i.e., $S = S_\omega \sin(\omega t)$. In that case (4.4) simplifies to

$$R = \epsilon^{-1}S_\omega[(\epsilon^{-1}\sigma)^2+\omega^2]^{-1}e^{-\epsilon^{-1}\sigma t}\{e^{\epsilon^{-1}\sigma\tilde{t}}[\epsilon^{-1}\sigma\sin(\omega\tilde{t}) - \omega\cos(\omega\tilde{t})]\}_{t=0}^{\tilde{t}=t}$$
$$= \epsilon^{-1}S_\omega[(\epsilon^{-1}\sigma)^2+\omega^2]^{-1}[\epsilon^{-1}\sigma\sin(\omega t) - \omega\cos(\omega t) + \omega e^{-\epsilon^{-1}\sigma t}]. \quad (4.5)$$

In this study we are not interested in the frequencies associated with lightning, but rather longer time phenomena such as those associated with the electrification of the cloud. Another way of saying this is that we are assuming that the high frequencies of S have negligible amplitudes so that the time scale of S is approximately that of the homogeneous solution at low altitudes, i.e., $\omega \approx \epsilon^{-1}\sigma$ ($r = r_{\text{ground}}$). Thus, we expect the solution at low altitudes to have only one time scale. Under this assumption $\omega \ll \epsilon^{-1}\sigma$ ($r = 0.5r_{\max}$) and at high altitudes we surmise that the solution will have two time scales. We will make this argument more rigorous in the discussion that follows. If S consisted solely of high frequencies $\omega \gg \epsilon^{-1}\sigma$ ($r = r_{\text{ground}}$) then at low altitudes the solution (4.5) would be well approximated by

$$R = -\epsilon^{-1}\omega^{-1}S_\omega[\cos(\omega t) - e^{-\epsilon^{-1}\sigma t}],$$

which is not the same as the solution obtained from (4.2a) by dropping the conduction current. The two solutions are approximately the same only if the product $\epsilon^{-1}\sigma t$ is large, i.e., at large times.

We now want to allow σ to be a function of r which is more realistic than the previous case. In this case we consider (4.1) with $n = 0$ which is the component of the solution with no θ variation. Equation (4.1) then becomes

$$(\sigma + \epsilon s)[\hat{E}_r + 2r^{-1}\hat{E}] + \sigma_r\hat{E} = \hat{S}, \quad (4.6)$$

where $\hat{E} = \hat{\phi}_r$. In physical space (4.6) can be written

$$[r^2(\sigma E + \epsilon E_t)]_r = r^2 S, \quad (4.7)$$

where $E = \phi_r$. We can integrate (4.7) in the form

$$\epsilon^{-1}\sigma E + E_t = \epsilon^{-1}r^{-2}[r^2(\sigma E + \epsilon E_t)]_{r=r_0} + \epsilon^{-1}r^{-2}\int_{r_0}^{r}\tilde{r}^2 S d\tilde{r}, \quad (4.8)$$

where r_0 is the starting point of the integration. Now (4.8) is just an inhomogeneous ordinary differential equation for E. The homogeneous solution of (4.8) which represents the reaction of the atmosphere to a net space charge in the case of no forcing mechanism is

$$E_h = E_h(t=0)e^{-\epsilon^{-1}\sigma t}, \quad (4.9)$$

and E_h decays with a time constant of $\epsilon\sigma^{-1}$. The homogeneous solution decays much faster at higher altitudes than near the ground as we surmised in the previous case. We will discuss the influence this fact has on the design of a numerical model in the next section.

The solution of (3.14) does not necessarily behave like (4.9) as there is also a component which arises from forcing terms on the right-hand side of (4.8). As in the case of constant σ the forcing term has a time constant of its own and this can completely alter the time dependence of the solution. To see this let us choose a starting point for the integration of (4.7) that is above the storm, i.e., we choose r_0 so that S is zero for all $r \geq r_0$. Define G as

$$G = \epsilon^{-1}r^{-2}[r^2(\sigma E + \epsilon E_t)]_{r=r_0}. \quad (4.10)$$

Then a particular solution of (4.8) is

$$E_p = e^{-\epsilon^{-1}\sigma t}\int_0^t e^{\epsilon^{-1}\sigma\tilde{t}}G d\tilde{t}. \quad (4.11)$$

Let us assume that G is the product of a spatial variation times a single frequency, i.e., that $G = f(r)\sin(\omega t)$. In this case the particular solution (4.11) becomes

$$E_p = f(r)[(\epsilon^{-1}\sigma)^2+\omega^2]^{-1} \times [\epsilon^{-1}\sigma\sin(\omega t) - \omega\cos(\omega t) + \omega e^{-\epsilon^{-1}\sigma t}]. \quad (4.12)$$

At high altitudes the homogeneous solution and the last term on the right-hand side of (4.12) tend to zero extremely fast and we are left with the solution

$$E_p = f(r)[(\epsilon^{-1}\sigma)^2+\omega^2]^{-1}[\epsilon^{-1}\sigma\sin(\omega t) - \omega\cos(\omega t)], \quad (4.13)$$

whose time scale is that of G and not the time scale of $\epsilon\sigma^{-1}$ of the homogeneous solution at high altitudes. Another way of saying this is that at high altitudes there is a component of the solution which has a time scale determined by the Maxwell current time variation just above the storm. We note that when lightning effects are neglected the time variation of the Maxwell current just above the storm is much slower than the time variation of the homogeneous solution at high altitudes so that we can further simplify (4.13) at these altitudes to

$$E_p = \frac{f(r)\sin(\omega t)}{\epsilon^{-1}\sigma}. \quad (4.14)$$

Note that at high altitudes the solution (4.14) is the steady state version of (4.8), i.e., it can be obtained directly from (4.8) by deleting E_t and then solving for E.

From the homogeneous solution (4.9) the ratio between the conduction current and the displacement current is

$$\frac{\sigma E_h}{\epsilon E_{ht}} = -1, \quad (4.15)$$

i.e., a constant. But for the solution (4.14) the ratio is given by

$$\frac{\sigma E_p}{\epsilon E_{pt}} = \frac{\sigma}{\epsilon\omega\cot(\omega t)}, \quad (4.16)$$

for nonzero values of $\cot(\omega t)$. As altitude increases σ increases exponentially so that for the particular so-

lution the ratio increases sharply. In the design of our numerical method we will assume that at high altitudes one is only interested in solutions of (3.14) given by (4.14) and expect solutions with properties closer to (4.16) than (4.15).

There is one additional property of the one-dimensional solution that we want to mention. Differentiating (4.12) with respect to time and setting the result to zero, we find that the abscissa of a local maxima or minima of E_p must satisfy the transcendental equation

$$\cos(\omega t) + \epsilon\omega\sigma^{-1}\sin(\omega t) - e^{-\epsilon^{-1}\sigma t} = 0. \quad (4.17)$$

The feature of interest is that since σ varies with altitude, the solutions t_m will depend on σ, i.e., the phase of the solution will depend on altitude. The homogeneous solution (4.9) does not have this property. Since the case $n = 0$ is one component of the full solution, we expect to see phase shifting in the two-dimensional case.

We now want to relax the assumption that $n = 0$. In this case we can only describe some features of the solution at high altitudes. Since we are only interested in solutions with a time scale much larger than that of the homogeneous solution at high altitudes, near the highly conducting region we can neglect the displacement current. We also assume that the storm is confined to lower altitudes. With these assumptions we can consider (4.1) with $s = S = 0$ which then becomes

$$\hat{\phi}_{rr} + 2(r^{-1} + 0.5\sigma^{-1}\sigma_r)\hat{\phi}_r - r^{-2}n(n+1)\hat{\phi} = 0. \quad (4.18)$$

If exponential conductivity is assumed then $\sigma^{-1}\sigma_r$ is constant. Freezing the remaining coefficients we can solve (4.18) by finding the characteristic roots given as solutions of the quadratic equation

$$z^2 + 2(r^{-1} + 0.5\sigma^{-1}\sigma_r)z - r^{-2}n(n+1) = 0.$$

The solution that stays bounded as $r \to \infty$ is

$$\hat{\phi} = \hat{\phi}(r = r_0)e^{-(r^{-1}+0.5\sigma^{-1}\sigma_r)-[(r^{-1}+0.5\sigma^{-1}\sigma_r)^2+r^{-2}n(n+1)]^{1/2}},$$

when r_0 is sufficiently high. Note that although there is damping of the components of the solution for all n, the damping increases with increasing n. Thus, we expect that the high-altitude solutions of interest will become independent of latitude, i.e., the mode $n = 0$ has the least damping and will be the dominant mode as altitude increases. This fits well with the physical situation. Since the conductivity increases with altitude, we expect the currents to flow upward and to spread horizontally at the height of greatest conductivity much as in the solutions for the quasi-static model discussed by Hays and Roble (1979), Roble and Hays (1979), and Tzur and Roble (1985).

5. Accuracy of the numerical method

As we have indicated in section 2 σ varies from a value of 3×10^{-14} mho m^{-1} at the ground to a value of 10^{-4} mho m^{-1} at the center of the highly conducting layer. For a typical explicit scheme the stability requirement is

$$\epsilon^{-1}\max_r[\sigma(r)]\Delta t \leq 1,$$

where $\epsilon = 10^{-11}$ mho s m^{-1} and Δt is the time step. If we used an explicit scheme then we would have to use a time step on the order of $\Delta t \approx 10^{-7}$ s. Since we are interested in electrical events with a time scale on the order of one minute this means that we would have to solve approximately 6×10^8 elliptic equations for each simulation. Clearly this would be prohibitive and so we consider an implicit scheme. The scheme for the full equation (3.14) is described in Appendix. Here we want to consider the effect of choosing an implicit scheme and it suffices to consider the constant coefficient case. As we have seen in section 4 in that case we can solve for the time dependence of the solution by solving the simple ordinary differential equation

$$u_t + \epsilon^{-1}\sigma u = f(t) \quad (5.1a)$$

with the initial condition

$$u(t = 0) = 0. \quad (5.1b)$$

We approximate (5.1) by the backwards Euler method which is given by

$$\frac{v^{n+1} - v^n}{\Delta t} + \epsilon^{-1}\sigma v^{n+1} = f^{n+1} \quad (5.2a)$$

with the initial condition

$$v^0 = 0, \quad (5.2b)$$

where $v^n = v(n\Delta t) \approx u^n = u(n\Delta t)$. Solving for v^{n+1} we can write (5.2a) in the form

$$v^{n+1} = \lambda(v^n + \Delta t f^{n+1}), \quad (5.3)$$

where

$$\lambda = (1 + \epsilon^{-1}\sigma\Delta t)^{-1}.$$

As is well known the backwards Euler method is unconditionally stable for the case that ϵ and σ are positive since then $0 < \lambda \leq 1$. Substituting u into (5.2a) we obtain the equation

$$u^{n+1} = \lambda(u^n + \Delta t f^{n+1} + \Delta t\tau^{n+1}), \quad (5.4)$$

where

$$\tau^{n+1} = -0.5\Delta t u_{tt}(t = t')$$

and $t^n \leq t' \leq t^{n+1}$. It is also well known that the backwards Euler method is consistent which can be seen in (5.4) since $\tau = O(\Delta t)$. Thus, by Lax's Equivalence Theorem we know that as $\Delta t \to 0$ the finite difference solution will converge to the solution of (5.1).

The error in the finite difference solution depends on the size of Δt. Let $e^n = u^n - v^n$. Then by subtracting (5.3) from (5.4) we find that e^n satisfies the equation

$$e^{n+1} = \lambda(e^n + \Delta t\tau^{n+1}) \quad (5.5a)$$

with the initial condition

$$e^0 = 0. \tag{5.5b}$$

The solution of (5.5) is

$$e^n = \lambda\Delta t(\tau^n + \lambda\tau^{n-1} + \cdots + \lambda^{n-1}\tau^1).$$

We can bound the error as

$$|e^n| \leqslant t \max_{1\leqslant k\leqslant n} |\tau^k|, \tag{5.6}$$

where $t = n\Delta t$. The bound in (5.6) is just the proof of convergence of the finite difference scheme as stated above. Let us consider the error bound given in (5.6) in the homogeneous case where the solution is given by

$$u = u(t=0)e^{-\epsilon^{-1}\sigma t}.$$

The bound in this case becomes

$$|e^n| \leqslant 0.5t\Delta t(\epsilon^{-1}\sigma)^2|u(t=0)|.$$

After one time step the error bound is

$$|e^1| \leqslant 0.5(\epsilon^{-1}\sigma\Delta t)^2|u(t=0)|.$$

If $\epsilon^{-1}\sigma\Delta t < 1$ (compare with the restriction on the time step for the explicit scheme) then the error is small. If $\epsilon^{-1}\sigma\Delta t > 1$ the error bound is large and the approximation might be inaccurate. Thus we expect that near the ground our approximation is accurate, but in the vicinity of the highly conducting layer it might be totally incorrect. However, this does not mean that the approximation is useless. The general solution is composed of the homogeneous solution plus a particular solution. If f is sufficiently smooth in time, then the particular part will have a small time derivative and the bound again becomes meaningful. To make this rigorous let us define $u = v = f = 0$ for $t < 0$ and assume f is square integrable. Fourier transforming (5.1) and (5.2) with respect to time we obtain

$$(i\omega + \epsilon^{-1}\sigma)\hat{u} = \hat{f} \tag{5.7}$$

$$\left(\frac{1 - e^{-i\omega\Delta t}}{\Delta t} + \epsilon^{-1}\sigma\right)\hat{v} = \hat{f}, \tag{5.8}$$

where ω is the real dual variable of t and the hat notation indicates the transform of a variable. Subtracting (5.8) from (5.7) the relative error is

$$|\hat{u}|^{-1}|\hat{u} - \hat{v}| = \left|\frac{1 - e^{-i\omega\Delta t}}{\Delta t} + \epsilon^{-1}\sigma\right|^{-1}\left|\frac{1 - e^{-i\omega\Delta t}}{\Delta t} - i\omega\right|$$

$$\leqslant (\epsilon^{-1}\sigma)^{-1}\left|\frac{1 - e^{-i\omega\Delta t}}{\Delta t} - i\omega\right|.$$

As we have seen earlier there is convergence of the finite difference solution to the true solution as $\Delta t \to 0$.

For fixed Δt the error is small as long as $(\epsilon^{-1}\sigma)^{-1}\omega^2\Delta t$ is small. We want to choose Δt so that $\epsilon^{-1}\sigma$ (10 km) $\Delta t \leqslant 1$, but $\epsilon^{-1}\sigma(0.5r_{\max})\,\Delta t \gg 1$. As we surmised earlier, in general the error is not small. For example choose $\omega = \epsilon^{-1}\sigma(0.5r_{\max})$ and σ to be its value at $r = 0.5r_{\max}$. Then the error is on the order of $\epsilon^{-1}\sigma(0.5r_{\max})\Delta t$ which by assumption is large. However, if we restrict ourselves to solutions with time derivatives which satisfy $\omega \leqslant \epsilon^{-1}\sigma$ (10 km) then the error is small throughout the region. Of course, in general all frequencies will be present and we really only need to require that the amplitudes of the high frequencies be sufficiently small so that they may be neglected. This will be true if f is sufficiently smooth in time.

6. Numerical results

The electrically active region of the cloud is defined, in this model, by a source function that has characteristics similar to observations. This source function separates charge and generates a dipole-type space charge with the positive charge center above the negative center. The magnitude of the source function S, which has units of $C\,m^{-3}\,s^{-1}$, can be approximated by relating it to the amount of charge that has been observed to be separated during the period between consecutive lightning bolts. According to various measurements (e.g., Simpson and Robinson, 1941; Gish and Wait, 1950; Malan, 1963; Kasemir, 1965, 1983; Jacobson and Krider, 1976) the magnitude of the charge separation in individual thunderstorms can range between 30° and 400°C.

To estimate a typical source function, we use estimates of the global lightning frequency and the number of active thunderstorms. We use estimates of the global lightning frequency that range between 40 to 140 s^{-1} (Orville and Spenser, 1979; Turman and Edgar, 1982; Kotaki and Katoh, 1983). The number of thunderstorms acting together at any time is about 2000 (Mühleisen, 1977), and, therefore, a typical thunderstorm should produce lightning every 15 to 50 s. According to this data, if we assume that 50°C are separated during 25 s then the volume integral of a typical source function should separate 2°C s^{-1}.

As an initial test of the model, we examine only one case study which is represented by the parameterized source function S given by

$$S(r,\theta) = f(r,\theta)g(t), \tag{6.1}$$

where f represents the spatial distribution function and g the time variation of the source. The spatial distribution is similar to the form used by Tzur and Roble (1985):

$$f(r,\theta) = A(e^{-[(r-r_p)/u]^2} - e^{-[(r-r_n)/u]^2})e^{-(r\theta/\omega)^2}, \tag{6.2}$$

where A is the amplitude, r is the vertical distance, r_n = 5 km is the negative charge center, r_p = 10 km is the positive charge center, and u = 1 km is the e-folding vertical width. The factor $e^{-(r\theta/\omega)^2}$ gives the horizontal distribution, where θ is in radians and ω = 2 km is the horizontal e-folding distance. The amplitude A is adjusted to produce an assumed electric field. Here, we

used $A = 10^{-10}\,\mathrm{C\,s^{-1}\,m^{-3}}$, which produces a maximum electric field of several kV $\mathrm{cm^{-1}}$ at the cloud center and produces a total current output of about 1 A. For the time-dependent part of the source function we assume

$$g(t) = 1 - e^{-t/\tau}, \tag{6.3}$$

where t is in seconds and $\tau = 100$ s. This function represents an electrification process which increases rapidly and then slows in response to possible saturation. This parameterization is actually a simplified choice and is used as a case study for ease in illustrating the basic model response. The charge separation current can be calculated from Eq. (2.2) after integrating over the source function.

As a storm is a small-scale feature in relation to its global environment, the independent variables are transformed to obtain more resolution in the vicinity of the cloud. The horizontal distance between the first two mesh points is several meters, while far from the storm the distance grows to several thousand kilometers. In the vertical direction we used a resolution of 0.5 km.

The calculated conduction and displacement currents at 100 s after the source function was applied to separate charge are shown in Figs. 1 and 2. The charge separation current at this time and near the center of the storm was 7.5×10^{-8} A $\mathrm{m^{-2}}$. Above the storm the horizontal current spreading into the global circuit decreases with altitude up to about 60 km and then increases abruptly where the electrical conductivity increases within the equalization layer and an almost equal ionospheric potential is obtained. The vertical current flows upward towards the equalization layer in a rather narrow tube. At 100 s after the source function was applied the displacement current is smaller than the conduction current and decreases very rapidly with altitude. Above the thunderstorm the output current has the same pattern as in the quasi-static case (Tzur and Roble, 1985).

Figure 3 shows the components of the electric field at 100 s. The maximum horizontal electric field at this time is 90 kV $\mathrm{m^{-1}}$ and the corresponding maximum of the vertical electric field is 200 kV $\mathrm{m^{-1}}$ which is close to the critical value for lightning to occur. Near the ground the vertical electric field reaches a maximum which is about one order of magnitude larger than the measured maximum underneath a thunderstorm (e.g., Standler, 1980; Standler and Winn, 1979). This discrepancy occurs because corona currents which limit the maximum field strength are not considered in this numerical experiment.

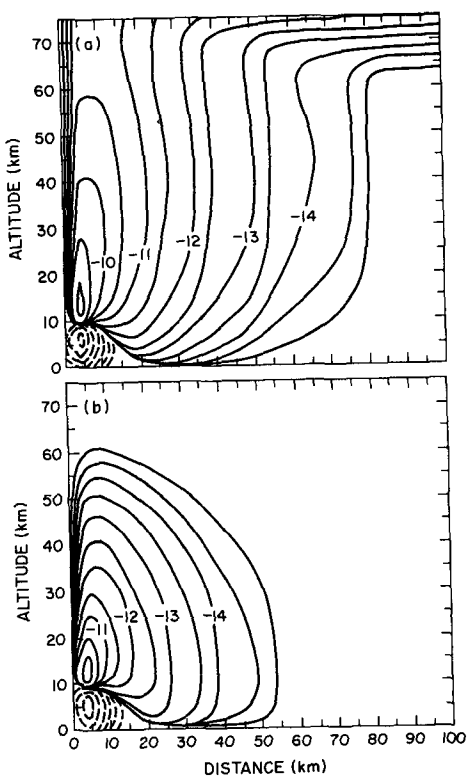

FIG. 1. Contours of $\log_{10} J$ (A $\mathrm{m^{-2}}$) at 100 s: (a) the horizontal conduction current and (b) the horizontal displacement current. Solid and dashed contours indicate current flowing away from and toward the storm center, respectively.

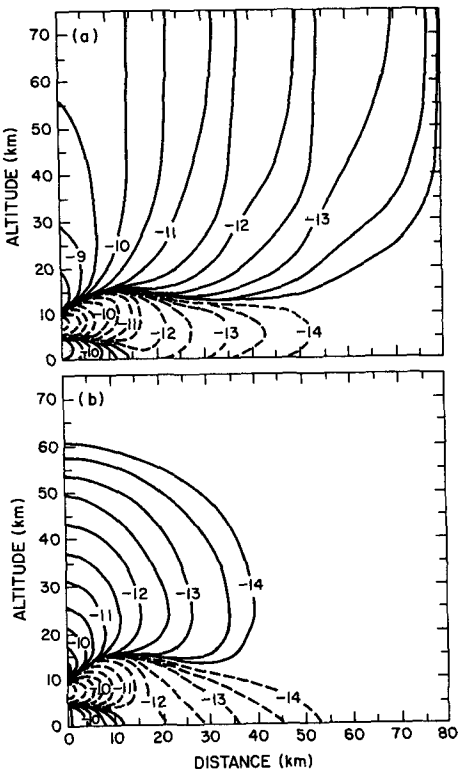

FIG. 2. As in Fig. 1, except the currents are the vertical component. Solid and dashed contours indicate currents flowing upward toward the ionosphere and downward toward the ground, respectively.

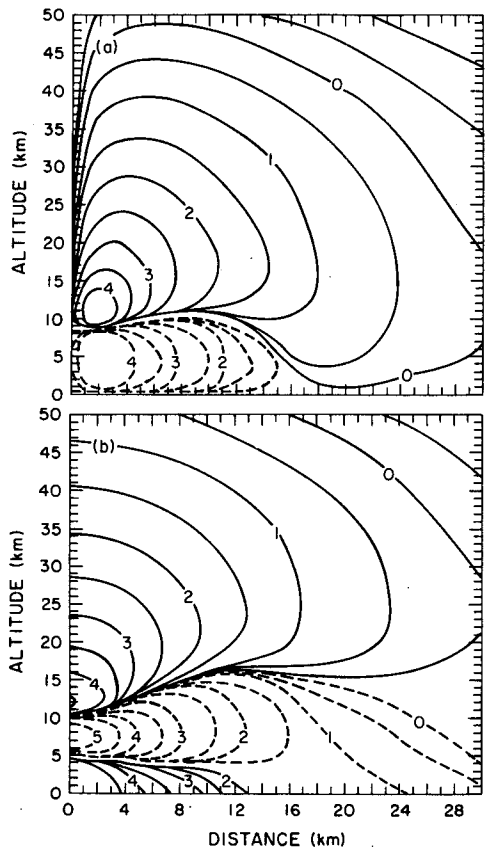

FIG. 3. Contours of $\log_{10}E$ (V m^{-1}) at 100 s: (a) the horizontal electric field and (b) the vertical electric field. Solid and dashed lines indicate positive and negative values, respectively.

Figure 4 shows the ratio of the conduction current to the displacement current as a function of altitude near the center of the storm. To demonstrate more rapid variations with time than that considered in previous case, we chose $\tau = 60$ s. The different curves in Fig. 4 correspond to different simulation times after the source function was applied. The perturbations from the monotone increase with altitude at about 4 and 10 km are produced by the space charge centers. The displacement current near the ground dominates during the initial charge buildup phase and then decreases with time. For $t \gg \tau$ the displacement current goes to zero and the conduction current dominates. The mathematical behavior of this solution has been discussed previously in section 4.

The analysis of the inhomogeneous solution of the model equation, discussed in section 4, indicates a phase shift between the source function and the two dimensional solution at various altitudes [see (4.17)]. To illustrate this phase shift we use a sinusoidal source function to represent the time variation. This source function is arbitrarily specified and it does not represent a real thunderstorm source current, but it has been chosen to illustrate the physical nature of the phase shift. It represents one component of the solution and demonstrates the phase shift as a function of altitude (conductivity). Figure 5 shows the calculated vertical electric field as a function of time at various altitudes. The calculated electric field at the center of the cloud is shown in Fig. 5a and at a distance of 250 km in Fig. 5b. A phase shift in time with respect to altitude is shown in both figures. The phase shift between the ground and 12 km is about 20 s for both cases. The results indicate that the electrical response of the atmospheric environment to a time varying source function is different at different altitudes. Therefore, measurements of electric field variations at different altitudes, such as from the ground and at balloon altitudes, may have a different temporal behavior.

7. Summary and discussion

The purpose of this paper is to introduce a time dependent model that can be used to simulate the interaction of a thunderstorm with its global electrical environment. The model solves the continuity equation of the Maxwell current which is assumed to be composed of the conduction, displacement, and source currents. Lightning phenomena are not considered and the electric field is assumed to be curl-free. The mechanism by which charge is separated inside the storm is represented by a bipolar source function.

We first apply the energy method to the continuity equation in order to determine boundary conditions that are sufficient to form a well posed initial–boundary value problem. This ensures that the physical solution exists and depends continuously on the initial and boundary data. To gain insight into the nature of the solutions of the initial–boundary value problem, we assume that the conductivity profile is only a function of altitude. Then we can apply analytic techniques to

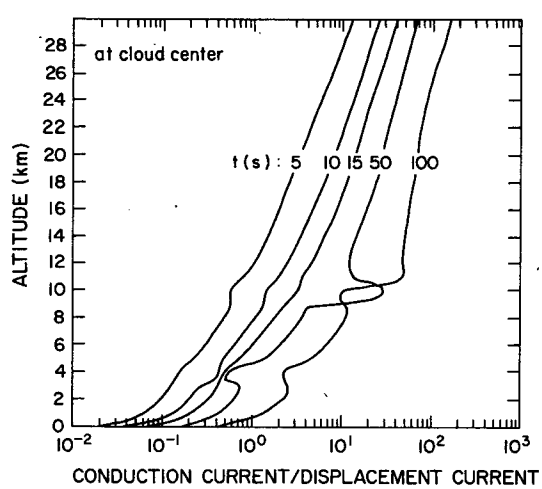

FIG. 4. The ratio $\sigma E(\epsilon E_t)^{-1}$ at the cloud center plotted as a function of altitude. The time since the source function was first applied appears on the corresponding curve.

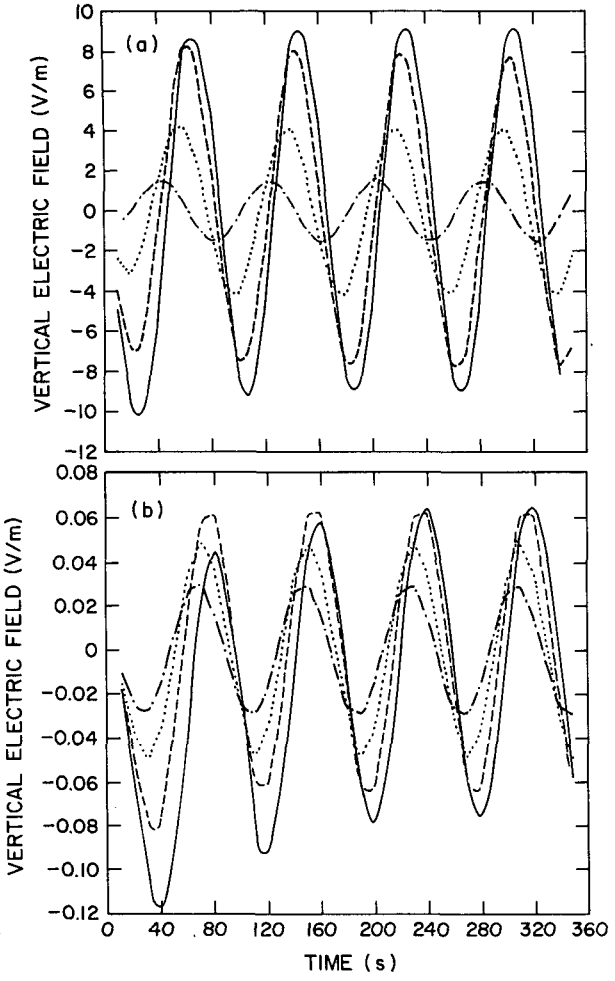

FIG. 5. The vertical electric field (a) at the center of the cloud and (b) at a distance of 250 km from the center of the cloud plotted as a function of time. The solid, dashed, dotted, and dash-dotted lines correspond to altitudes of 0 km, 4 km, 8 km and 12 km.

study the dependence of the solution on the properties of the medium such as the permitivity, conductivity profile, and the source function S. We find that the solution has two time scales, one determined by the ratio of permitivity over the conductivity and the other by the time scale of the source function S. It is shown that the two components of the solution have very different properties. For example, the ratio of the conduction current over the displacement current is constant for the homogeneous solution, while for the particular solution the same ratio increases exponentially with altitude. The presence of a source function can cause time phase shifting of the solution which depends on altitude.

In general, we do not want to restrict ourselves to a conductivity profile that is only a function of altitude. Then we must resort to a numerical method to solve the continuity equation. Since the conductivity increases sharply with altitude, we can not hope to compute a solution in a time interval on the order of tens of minutes unless an implicit method is used. We introduce such an implicit method and discuss the implications that the method has on the form of the source function S. The numerical results are compared with the analytic results obtained for the special case of a conductivity profile which only depends on altitude.

The analytic and numerical results demonstrate the important role that the displacement current plays in the electrical interaction between a thunderstorm and its environment during the initial charge buildup phase of a developing thunderstorm. Beneath the storm the displacement current dominates the conduction but relaxes to zero as a quasi-static state is approached. Above the thunderstorm conduction current dominates and the total current flowing to the ionosphere follows the time history of the changing source function.

About 1 A of current flows from the storm model into the global circuit for the quasi-static case where $t \gg \tau$. This current flows in a narrow column toward the ionosphere and spreads globally in the equalization layer. The current returns to the ground in the fair weather region which extends to distances above about 100 km away from the storm center. A similar structure was calculated by the quasi-static model of Tzur and Roble (1985). The time-dependent simulation shows, however, that displacement currents will interact with the storm's electrical environment whenever charge adjustment process occurs. Thus, the total Maxwell current has components of charge separation current, displacement current, and conduction current that vary in a complex manner over the life history of a thunderstorm.

In this initial study we concentrated primarily on the theoretical analysis and the mathematical properties of the model and demonstrated model performance for a relatively simple case. In part 2 a more detailed analysis of the thunderstorm physical processes and its interaction with the global electrical environment will be presented.

Acknowledgments. This research was partially supported by NASA Grants W-15 028 and NAGW-772.

APPENDIX

Although the mathematical analysis of section 4 gives us considerable insight into the nature of the solutions of (3.14), we can not obtain full details of the two dimensional solution without using numerical methods. The selection of the numerical method we used to obtain the results in section 5 was based on the well known concept that finite differences can always be chosen so that the energy method to prove stability will closely follow the energy method used to prove well posedness. As might be expected from this reasoning the proof of stability holds in three dimensions, but to simplify the presentation we will restrict ourselves to the two-dimensional case.

To discretize the two-dimensional equation (3.14) we choose spatial increments $\Delta\theta = \pi/2(J-2)$ and $\Delta r = r_{\max}/(K-1)$ where J and K are positive integers. The temporal increment Δt will be determined by the stability requirement. In the two-dimensional case the proper grid to be used for the energy method is given by

$$G = \{(\theta_j, r_k, t_n): \theta_j = (j-0.5)\Delta\theta, \quad r_k = (k-1)\Delta r, t_n = n\Delta t\},$$

where $1 \leqslant j \leqslant J$, $1 \leqslant k \leqslant K$, and $n \geqslant 0$. We employ the standard grid function notation that $\phi^n_{j,k} \approx \phi(\theta_j, r_k, t_n)$. When subscripts or superscripts are missing on a grid function it is to be assumed that they are their nominal values j, k, or n as appropriate. We define the difference operators

$$D_{-\theta}\phi = \frac{\phi_j - \phi_{j-1}}{\Delta\theta}, \quad D_{+\theta}\phi = \frac{\phi_{j+1} - \phi_j}{\Delta\theta},$$

$$D_{-r}\phi = \frac{\phi_k - \phi_{k-1}}{\Delta r}, \quad D_{+r}\phi = \frac{\phi_{k+1} - \phi_k}{\Delta r},$$

$$D_{-t}\phi = \frac{\phi^n - \phi^{n-1}}{\Delta t}.$$

We approximate the homogeneous version of (3.14) for $2 \leqslant j \leqslant J-1$, $2 \leqslant k \leqslant K-1$, and $n \geqslant 1$ by the backwards Euler method in time and centered second order differences in space which we can write as

$$\epsilon D_{-t}L(1,\phi) + L(\sigma,\phi) = 0, \tag{A1}$$

where

$$L(g,h) = r^{-2}[g \sin^{-1}\theta D_{-\theta}(\sin\theta D_{+\theta}h) + D_{-r}(r^2 g D_{+r}h)].$$

The numerical approximations to the boundary conditions (3.15a–d) are given by

$$\phi_{j,1} = 0 \quad (2 \leqslant j \leqslant J-1), \tag{A2a}$$

$$\phi_{j,K} = 0 \quad (2 \leqslant j \leqslant J-1), \tag{A2b}$$

$$D_{+\theta}\phi_{1,k} = 0 \quad (2 \leqslant k \leqslant K-1), \tag{A2c}$$

$$D_{+\theta}\phi_{J-1,k} = 0 \quad (2 \leqslant k \leqslant K-1). \tag{A2d}$$

Multiplying (A1) by $-\epsilon^{-1}\Delta t(\phi^n + \phi^{n-1})r^2 \sin\theta$ and then summing over all interior spatial grid points we have

$$-\sum_{k=2}^{K-1}\sum_{j=2}^{J-1}(\phi^n + \phi^{n-1})r^2 \sin\theta[L(1,\phi^n) - L(1,\phi^{n-1}) + \epsilon^{-1}\Delta t L(\sigma,\phi)] = 0. \tag{A3}$$

In the continuous case we used integration by parts. Here we have the summation by parts formula

$$-\sum_{k=2}^{K-1}\sum_{j=2}^{J-1} fr^2 \sin\theta L(g,h) = \sum_{k=2}^{K-1}\sum_{j=1}^{J-1} g \sin\theta[D_{+\theta}f][D_{+\theta}h] + \sum_{k=1}^{K-1}\sum_{j=2}^{J-1} r^2 g \sin\theta[D_{+r}f][D_{+r}h], \tag{A4}$$

where f and h are any grid functions that satisfy the boundary conditions (A2) and g is only dependent on r_k. Using (A4) we can rewrite (A3) as

$$\|\phi^n\| \leqslant \|\phi^{n-1}\|, \tag{A5}$$

where

$$\|\phi^n\| = \sum_{k=2}^{K-1}\sum_{j=1}^{J-1}(1 + 0.5\epsilon^{-1}\sigma\Delta t)\sin\theta[D_{+\theta}\phi^n]^2 + \sum_{k=1}^{K-1}\sum_{j=2}^{J=1}(1 + 0.5\epsilon^{-1}\sigma\Delta t)r^2 \sin\theta[D_{+r}\phi^n]^2.$$

Equation (A5) is an estimate on the differences of ϕ analogous to the estimate on the derivatives of ϕ given in (3.11). Since there is a finite difference analog of (3.5), Eq. (A5) states that the finite difference scheme (A1) in conjunction with the boundary conditions (A2) is unconditionally stable.

In section 3 we assumed that a solution exists and then proved that it must satisfy (3.13). Using the methods above for the strip problem we can obtain bounds on ϕ and differences of ϕ of all orders. Using the same techniques that are used to prove the existence of solutions of symmetric hyperbolic systems, these estimates can be used to prove the existence of a solution of (3.14) for the strip problem.

REFERENCES

Anderson, F. J., and G. D. Freier, 1969: Interaction of the thunderstorm with a conducting atmosphere. *J. Geophys. Res.*, **74,** 5390–5396.

Blakeslee, R. J., and E. P. Krider, 1981: Measurements of current densities under Florida thunderstorms. *Eos,* **62,** 881.

——, and ——, 1982: Maxwell current patterns under thunderstorms. *Eos,* **63,** 892.

——, and ——, 1983: The horizontal variation of the Maxwell current density under Florida thunderstorms. *Eos,* **64,** 661.

Boström, R., and U. Fahleson, 1977: Vertical propagation of time-dependent electric fields in the atmosphere and ionosphere. *Processes in Atmospheres,* Steinkopff Verlag, 529–534.

Browning, G., A. Kasahara and H.-O. Kreiss, 1980: Initialization of the primitive equations by the bounded derivative method. *J. Atmos. Sci.,* **7,** 1424–1436.

Courant, R., and D. Hilbert, 1966: *Methods of Mathematical Physics, Vol. 1,* Interscience.

Gish, O. H., and R. G. Wait, 1950: Thunderstorms and the earth's general electrification. *J. Geophys. Res.,* **55,** 473–484.

Hays, P. B., and R. G. Roble, 1979: A quasi-static model of global atmospheric electricity, 1, The lower atmosphere. *J. Geophys. Res.,* **84,** 3291–3305.

Holzer, R. E., and D. S. Saxon, 1952: Distribution of electrical conduction currents in the vicinity of thunderstorms. *J. Geophys. Res.,* **57,** 207–216.

Holzworth, R. H., M. C. Kelley, C. L. Siefring, L. C. Hale and J. D. Mitchell, 1985: Electrical measurements in the atmosphere and

the ionosphere over an active thunderstorm: II Electrical field and conductivity. *J. Geophys. Res.*, **90,** 9824–9830.

Illingworth, A. J., 1972: Electric field recovery after lightning as the response of the conducting atmosphere to a field change. *Quart. J. Roy. Meteor. Soc.*, **98,** 604–616.

Israel, H., 1973: Atmospheric Electricity. *Israel Program for Scientific Translations, Vol. 2,* 1973.

Jacobson, E. A., and E. P. Krider, 1976: Electrostatic field changes produced by Florida lightning. *J. Atmos. Sci.*, **33,** 102–117.

Kasemir, H. W., 1959: The thunderstorm as a generator in the global electric circuit. *Z. Geophys.*, **25,** 33–64.

——, 1965: The thundercloud. *Problems of Atmospheric and Space Electricity,* Elsevier, 215–231.

——, 1983: Charge distribution in thunderstorms. *Proceedings in Atmospheric Electricity,* A. Deepak, 125–132.

Kotaki, M., and C. Katoh, 1983: The global distribution of thunderstorm activity observed by the ionosphere sounding satellite (ISS-b). *J. Atmos. Terr. Phys.*, **45,** 833–841.

Krider, E. P., 1981: Thunderstorm currents. *Eos,* **62,** 881.

——, and J. A. Musser, 1982: Maxwell currents under thunderstorms. *J. Geophys. Res.*, **87,** 11 171–11 176.

——, and R. J. Blakeslee, 1985: The electric currents produced by thunderstorms. *J. Electrostatics,* **16,** 369–378.

Malan, D. J., 1963: *The Physics of Lightning.* English University Press.

Mann, Jr., J. E., 1970: Interaction of a thunderstorm with a conducting atmosphere. *J. Geophys. Res.*, **75,** 1697–1709.

Mühleisen, R., 1977: The global circuit and its parameters. *Electrical Processes in Atmospheres,* Steinkopff.

Nisbet, J. S., 1983: A dynamic model of thundercloud electric fields. *J. Atmos. Sci.*, **40,** 2855–2873.

——, 1985: Thundercloud current determination from measurements at the earth's surface. *J. Geophys. Res.*, **90,** 5840–5853.

Orville, R. E., and D. W. Spencer, 1979: Global lightning frequency. *Mon. Wea. Rev.*, **107,** 934–943.

Roble, R. G., and P. B. Hays, 1979: A quasi-static model of global atmospheric electricity. *J. Geophys. Res.*, **84,** 7247–7256.

Simpson, G. C., and G. D. Robinson, 1941: The distribution of electricity in thunderclouds, 2. *Proc. Roy. Soc.*, **A177,** 281–329.

Standler, R. B., 1980: Estimation of corona current beneath thunderclouds. *J. Geophys. Res.*, **85,** 4541–4553.

——, and W. P. Winn, 1979: Effects of coronae on electric fields beneath thunderstorms. *Quart. J. Roy. Meteor. Soc.*, **105,** 285–302.

Turman, B. N., and B. C. Edgar, 1982: Global lightning distributions at dawn and dusk. *J. Geophys. Res.*, **87,** 1191–1206.

Tzur, I., and R. G. Roble, 1985: The interaction of a dipolar thunderstorm with its global electric environment. *J. Geophys. Res.*, **90,** 5989–5999.